Monolithic Active Pixel Sensors for the Linear Collider ECal

James E. Brau[1,*], *Martin* Breidenbach[2], *Angelo* Dragone[2], *Alexandre* Habib[2], *Lorenzo* Rota[2], *Mirella* Vassilev[2], and *Caterina* Vernieri[2,**]

[1]University of Oregon, Eugene, OR USA
[2]SLAC National Accelerator Laboratory, Menlo Park, CA, USA

Abstract. Higgs factory detectors require unprecedented precision to fulfill their physics program. A linear collider (such as ILC, C3, and CLIC) enables this precision with low duty cycles, low backgrounds, and reach to the TeV center-of-mass energy. The SiD Collaboration Monolithic Active Pixel Sensor (MAPS) technology for tracking and electromagnetic calorimetry (ECal), will result in high granularity, thin sensors, good time resolution (<nsec), and small dead areas. Detailed simulation of ECal performance, based on the first MAPS prototype (NAPA-p1) designed by SLAC, confirms previous results, indicating electromagnetic energy resolution based on digital hit cluster counting provides improved performance over the SiD TDR analog design, with two particle separation to the millimeter scale in the ECal. Wafer-scale sensors are the long-term goal.

1 Introduction

Higgs factory experiments require high precision, including that of the electromagnetic calorimeter. Monolithic Active Pixel Sensors (MAPS) offer attractive capabilities in pursuit of this requirement. [1–3]. Low backgrounds can contribute to this capability, with the low duty cycles of linear colliders (such as ILC, C^3, and CLIC). The timing structures (Figure 1) enable this. The SiD Collaboration [4] is developing an application of Monolithic Active Pixel Sensors (MAPS) technology for its tracking and electromagnetic calorimetry (ECal) with high granularity, thin sensors, fast responses (<nsec), small dead areas, and gaseous cooling and passive heat removal enabled by the low linear collider duty cycle.

2 The prototype Monolithic Active Pixel Sensors (MAPS)

SLAC designed the first MAPS prototype of this effort (NAPA-p1, NAnosecond timing Pixel for large Area sensors — prototype1) in CMOS imaging 65 nm technology. The first prototype is 1.5 mm × 1.5 mm with a 25 μm pixel pitch [5]. The future goal involves development of a ∼ 5 cm × 20 cm wafer-scale sensor. Large area MAPS applications eliminate delicate and expensive bump-bonding, and enables better timing with a CMOS foundry process.

3 The SiD electromagnetic calorimeter (ECal)

Precision measurements of the Higgs boson, the W and Z bosons, the top quark and other particles have set the primary design goals for SiD [4]. The detector can be optimized for these precision measurements due to the relatively benign linear collider experimental conditions, including lower collision rates, lower complexity, and less background than experienced in a hadron collider. Excellent jet reconstruction and measurement drive the calorimetry requirements. Measurement of W and Z bosons in their hadronic decay modes motivates a PFA application with a goal of 3–4% jet mass resolution at energies above 100 GeV.

The longitudinal structure of the SiD ECal defined in the ILC TDR [6] remains unchanged. The ECal has thirty layers, twenty with 2.5 mm tungsten thickness and 1.25 mm readout gap, followed by ten with 5 mm tungsten plus the same 1.25 mm readout gap. This configuration yields 26 radiation lengths with good containment of high-energy electromagnetic showers.

The pixel geometry is defined by the tracking requirements. 25 μm × 100 μm (2500 μm^2 area) was initially chosen based on its tracking precision with the 25 μm size in the bend plane. Recent tracking considerations now favor 25 μm × 50 μm or 25 μm × 25 μm; the earlier segmentation is used in these studies. The scale of electromagnetic shower spreading and the resulting pixel activation yields excellent performance from a digital ECal compared to the coarser granular analog approach. Earlier studies [7–11] demonstrated potential digital ECal energy resolution advantages. Full calorimeter prototype beam tests have produced results consistent with expectations [10, 12].

SiD's design for the MAPS tracker and digital ECal requires 1364 m^2 of silicon, including 54 m^2 in the barrel tracker, 20 m^2 in the end cap tracker, 1000 m^2 in the barrel ECal, and 290 m^2 in the end cap ECal. The sparse readout of a very small fraction of the pixels operates between bunch trains without a trigger.

*e-mail: jimbrau@uoregon.edu
**e-mail: caterina@slac.stanford.edu

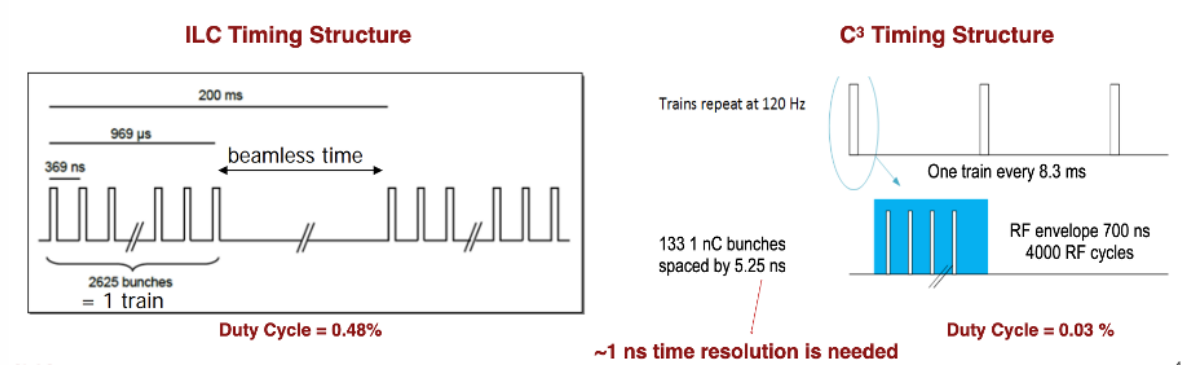

Figure 1. Linear Collider Timing Structure

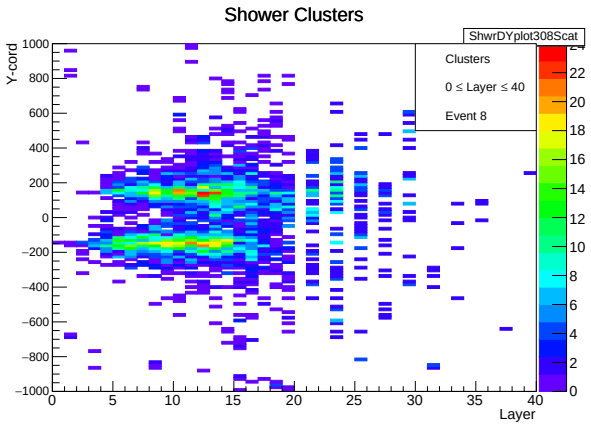

Figure 2. Projection of clusters in the 25 μm direction from 40 GeV $\pi^0 \rightarrow$ two 20 GeV γ's separated by 10 mm

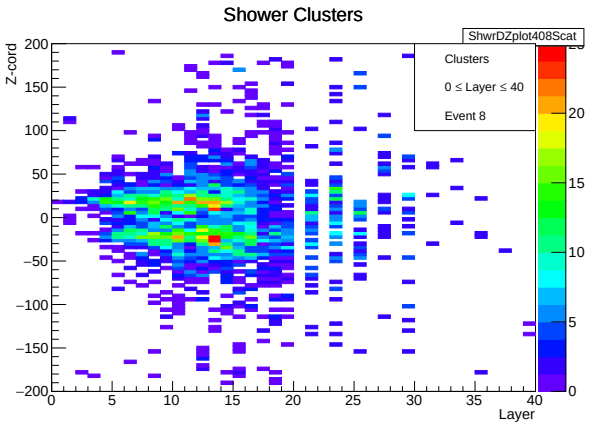

Figure 3. Projection of clusters in the 100 μm direction from 40 GeV $\pi^0 \rightarrow$ two 20 GeV γ's separated by 10 mm

4 Performance

GEANT4 simulation studies of the SiD design confirmed the earlier MAPS studies referred to in the ILC TDR and reveal performance details such as energy resolution even better than the SiD TDR analog design [13]. The simulation aims to determine the ultimate performance and limitations of the digital ECal, but also informs the ASIC designers on the sensor requirements. SiD's 5 Tesla magnetic field was found to have a minor effect on resolution, degrading it by a few per cent. The small pixels also significantly improve shower separation in the ECal, with showers and particle distinguishable down to the millimeter scale. This important feature improves hadron shower measurements with the particle flow technique,

Two-shower separation is illustrated for two 20 GeV gamma showers from a 40 GeV π^0 decay in Figures 2 and 3. Excellent separation is shown, enabled by the fine granularity of pixels. Identification of two showers down to the mm scale of separation is possible. The energy resolution of the showers degrades significantly only for showers within millimeters of separation.

To understand the details of the digital ECal performance, we first compare the number of pixels with energy deposition in the 12 μm of sensitive epitaxial layer above the threshold of about 1/4 MIP (MIP ~4 keV , including integration over angles of incidence), or 1 keV (referred to as Hits), and the number of particles with kinetic energies over 0.1 MeV passing through the sensors (referred to as MIPs). 20 GeV gammas in the SiD with the 5 Tesla field produce means of about 2500 Hits and 1400 MIPs. The energy deposition by electrons and positron with kinetic energy below the 0.1 MeV MIP threshold, delta ray production, gamma absorption, and pixel charge sharing for MIPs results in the larger Hits count over MIPs. The Hit count is the simplest detector measurement, without optimization considerations of the shower and hit properties, while the MIP count represents an ideal, potential signal. For 20 GeV gammas, the resolutions for Hits and MIPs are 4.2% and 2.0%. However, the experimental resolution can be improved using the details of the measured digital Hit distributions. The noise from electronics, which is not expected to significantly affect results, is ignored.

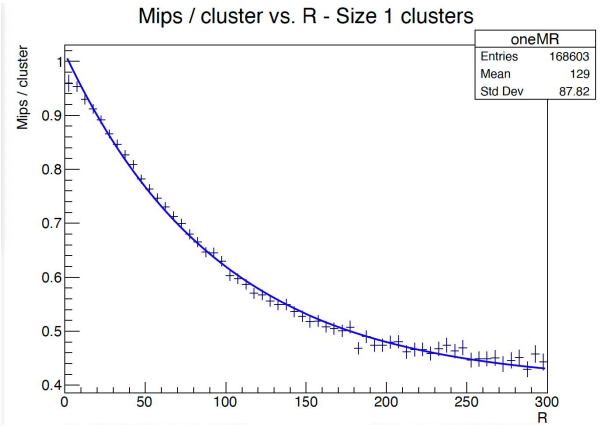

Figure 4. Mips per cluster for cluster size 1 versus the cluster's distance from the shower axis in 25 μm units.

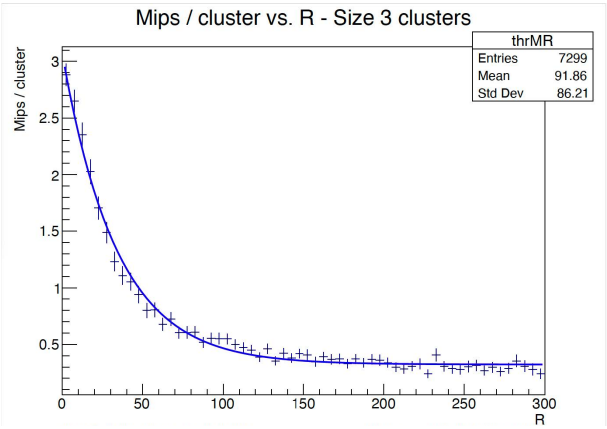

Figure 5. Mips per cluster for cluster size 3 versus the cluster's distance from the shower axis in 25 μm units.

Figure 6 summarize our results, which we now describe. The MIPS performance described above includes all MIPS ignoring the finite pixel size and the loss of resolution that results from the pile up of mips in a single pixel. All MIPS are shown as "ALL mips" in the figure and the mip count after considering single pixel pile up is shown as "mip active pixels" in the figure. When multiple mips in the same pixel are counted just once at 20 GeV, the GEANT4 simulations reduce the count of MIPS to about 1250 at 20 GeV and degrades the MIPS resolution to about 2.5%, still significantly better than the Hits performance.

An idealized goal is set by the MIPs performance. We seek an algorithm of the Hits which reaches as closely as possible to this ideal performance. An improvement in the count is achieved by combining Hits into clusters and counting clusters rather than all Hits. A cluster is constructed by combining all Hits that touch each other on any of the eight possibilities, boundaries or corners. Another improvement comes from observing the probability that multiple MIPs appear in clusters as a function of the cluster size and the cluster position in the shower, longitudinally and transversely. The transverse distribution is shown in Figures 4 and 5 for clusters made of just 1 Hit (size 1 clusters) and clusters made of 3 Hits (size 3 clusters). (The radius is shown in units of 25 μm, the smaller pixel scale.) Pileup of mips along the axis of the shower results in the maximized mips per cluster on axis, falling off away from the shower axis. The weighted clusters have a 20 GeV gamma resolution of 3.1%. The resulting energy-dependent resolution between 1 and 50 GeV is well characterized by 12.2%/ $\sqrt{E} \oplus 1.4\%$, compared to the MIP resolution of 9.8%/ $\sqrt{E} \oplus 1.1\%$.

The gamma energy resolution as a function of energy is displayed in Figure 6. The curves compare the ideal performance for basic MIP counting (light blue) to that achieved by optimizing the analysis of Hits in clusters with spatial weighting (dark blue). Future simulation studies will address optimized shower reconstruction and π^0s within jets, electromagnetic shower separation from other depositions in the ECal, and the impact of each on jet energy resolution, particularly for Higgs branching ratio measurements. The large volume of data provided by a MAPS-based ECal reveals details of particle showers which can be employed in Machine Learning analysis, which is being investigated.

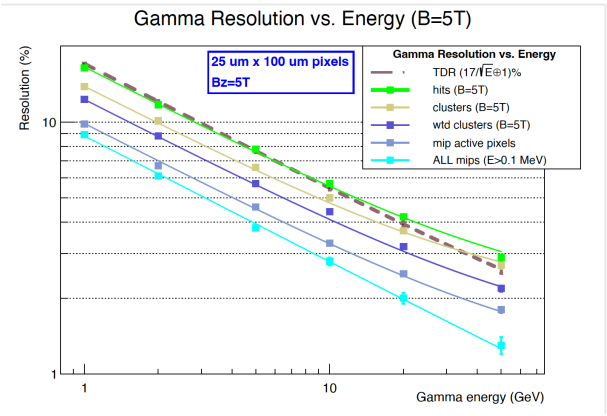

Figure 6. Energy resolution for gamma showers vs. energy: ALL mips: 8.8%/ $\sqrt{E} \oplus 0.2\%$; mips ac pix: 9.8%/ $\sqrt{E} \oplus 1.1\%$; wtd clusters: 12.2%/ $\sqrt{E} \oplus 1.4\%$; clusters 13.7%/ $\sqrt{E} \oplus 1.9\%$; Hits 16.4%/ $\sqrt{E} \oplus 2.0\%$; TDR 17%/ $\sqrt{E} \oplus 1.0\%$.

The future work studies will include:

- Potential of multi-bit digital operation;
- Jet reconstruction, including machine learning applications;
- Mechanical design of modules including heat removal;
- Optimization of the overall ECal design, including consideration of manufacturability, possible with robots.

5 Conclusion

The use of MAPS in the tracking and ECal systems of SiD will deliver significantly improved performance from that envisioned in the ILC TDR [6]. This application particularly improves speed and resolution performance. Recent, complementary results to those described here are presented in [14]. Large scale areas of silicon sensors will

be enabled at reasonable cost, benefiting future collider detectors requiring several hundred m^2 for low mass trackers and sampling calorimetry. This work is particularly driven by very thin, large areas with micron scale resolution requirements for trackers and calorimeters. The low duty cycle of linear colliders enables operation timed with the accelerator bunch train, with analog front-end circuitry powered off between bunch trains, reducing the power by more than two orders of magnitude. This power pulsing is being designed in the pixel front-end circuitry so the noise and timing performance of the circuitry can be optimized while maintaining low-power consumption. Development of wafer-scale MAPS will allow designers to investigate and optimize the power pulsing, power distribution, yield, stitching techniques, assembly and power delivery.

The SiD ECal simulation studies summarized here demonstrate the capability of MAPS to deliver the precision performance required for the Higgs Factory physics.

The authors were supported by the U.S. Department of Energy contract DE-AC03-76SF00515 and grant DE-SC0017996 for this research.

References

[1] "Exploring the Quantum Universe; Pathways to Innovation and Discovery in Particle Physics - Report of the 2023 Particle Physics Project Prioritization Panel". US Particle Physics.
https://www.usparticlephysics.org/2023-p5-report/

[2] "2020 Update of the European Strategy for Particle Physics,"
https://home.cern/sites/default/files/2020-06/2020

[3] "The International Linear Collider: Report to Snowmass 2021," arXiv:2203.07622 [physics.acc-ph]

[4] https://pages.uoregon.edu/silicondetector/; silicondetector.org

[5] Habib, A.; et al. "NAPA-p1: monolithic nanosecond timing pixel for large area sensors, designed for future e^+e^- colliders," JINST 19 (2024) 04, C04033.

[6] Behnke, T.; et al., "The International Linear Collider Technical Design Report - Volume 4: Detectors," arXIV:1306.6329[physics.ins-det].

[7] Ballin, J.A.; et al. "A Digital ECAL based on MAPS," arXiv:0901.4457.

[8] Stanitzki, M.; SPiDeR Collaboration. "Advanced monolithic active pixel sensors for tracking, vertexing and calorimetry with full CMOS capability," *Nucl. Instrum. Methods Phys. Res. Sect. A Accel. Spectrometers Detect. Assoc. Equip.* **2011**, *650*, 178–183.

[9] Dauncey P.; SPiDeR Collaboration. "Performance of CMOS sensors for a digital electromagnetic calorimeter," *PoS* **2010**, *502*, ICHEP2010.

[10] De Haas, A.P.; et al. "The FoCal prototype—An extremely fine-grained electromagnetic calorimeter using CMOS pixel sensors," *J. Instrum.* **2018**, *13*, P01014.

[11] Brau, J.E.; et al. "The SiD Digital ECal Based on Monolithic Active Pixel Sensors," *Instruments***2022**, *6*, 4, 51.

[12] Alme, J.; et al. "Performance of the electromagnetic pixel calorimeter prototype Epical-2," *J. Instrum.***2023**, *18*, P01038.

[13] Steinhebel, A.; Brau, J. “Studies of the Response of the SiD Silicon-Tungsten ECal,” SLAC-econf-C161205.4. arXiv:1703.08605 [physics.ins-det].

[14] Brau, J.E.; et al "The SiD Digital ECal Based on Monolithic Active Pixel Sensors," EPJ Web of Conferences 315, 03005 (2024).